A Spatially filtered data from simulation $\mathcal{S}_\bullet$ and $\mathcal{S}_\circ$

Results from simulation $\mathcal{S}_\bullet$ and $\mathcal{S}_\circ$ after low-pass filtering are given here.

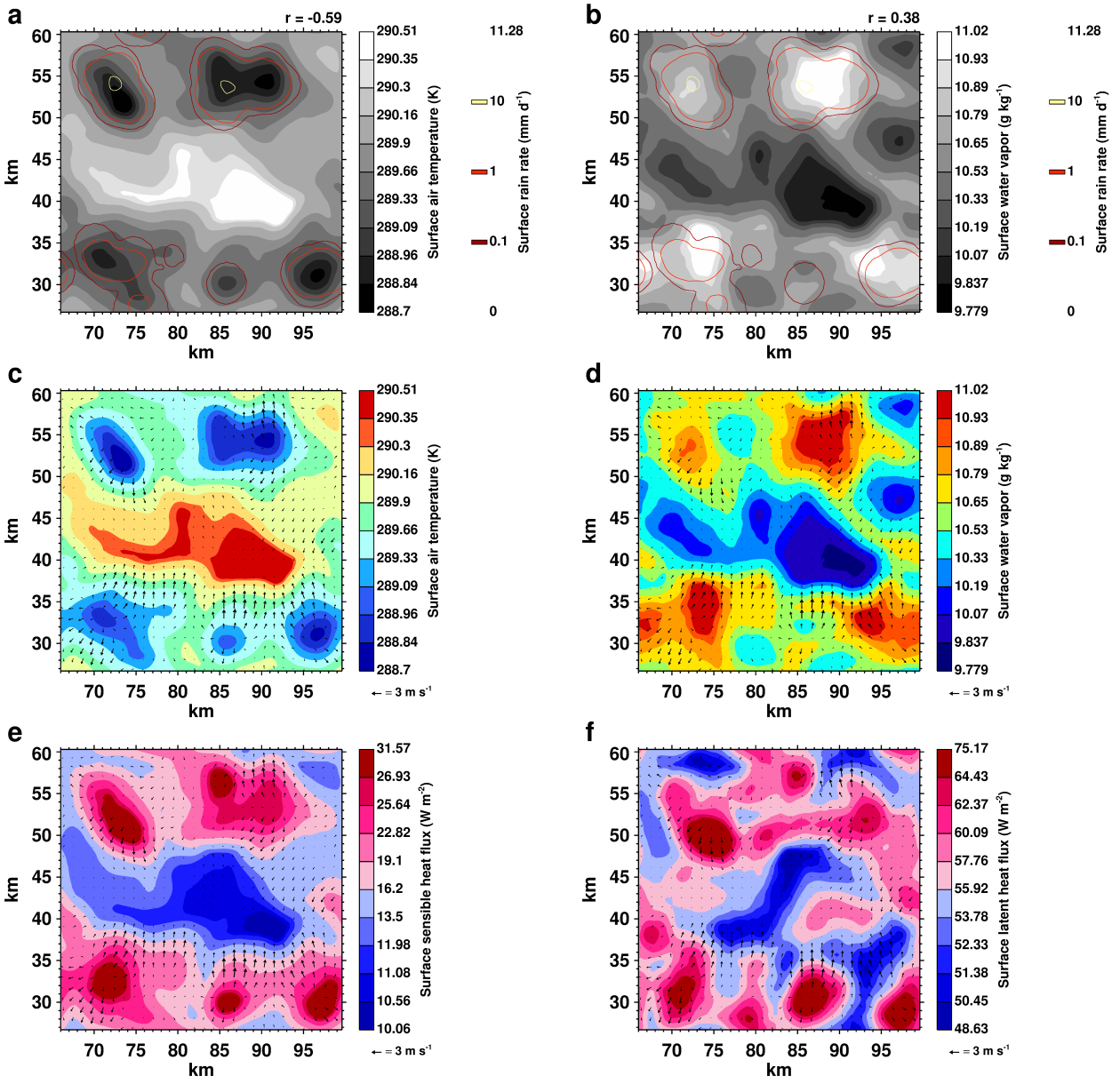

Fig. A-1. Surface air temperature (a) and water vapor (b) superimposed with the surface rain rate; surface air temperature (c) and water vapor (d) with the residual horizontal surface wind field; and the surface sensible (e) and latent (f) heat flux with the residual horizontal surface wind field, after applying a circular low-pass filter with a diameter of 4500 m, after 26 h in a select region of simulation $\mathcal{S}_\circ$. Domain-wide correlation coefficients are given for pairs of scalar quantities. Irregular contour intervals (at select percentiles of the data) are used for better visualization. Color scales are bounded by minima and maxima of the data. Minimum and maximum line contours are suppressed. The corresponding spatially unfiltered data are shown in Fig. 9.

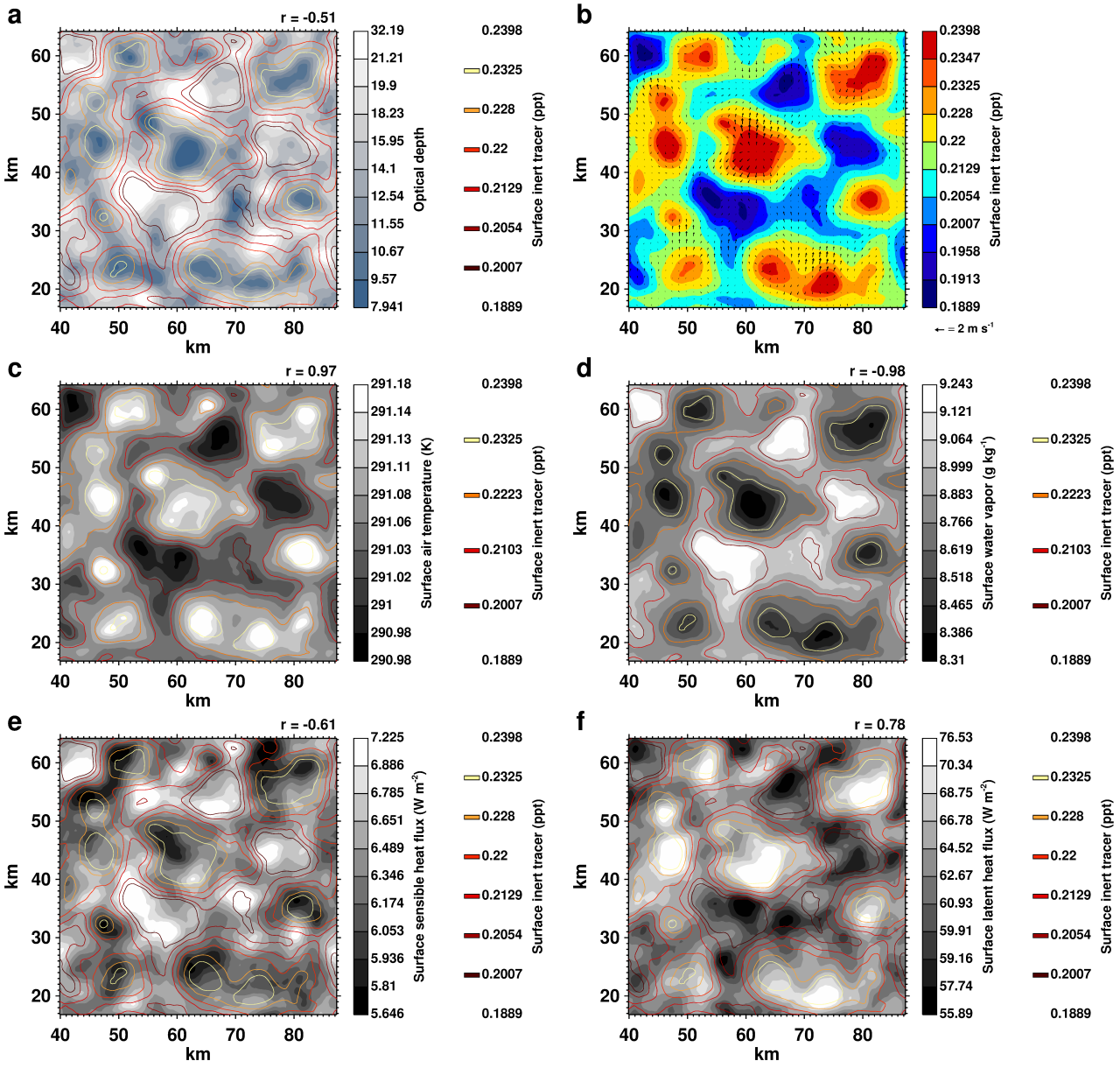

Fig. A-2. Surface mixing ratio of the inert tracer, with (a) cloud optical depth, (b) residual horizontal surface wind field, (c) surface air temperature, (d) surface water vapor, and surface sensible (e) and latent (f) heat flux, after applying a circular low-pass filter with a diameter of 4500 m, after 12 h in a select region of simulation $\mathcal{S}_\bullet$. Domain-wide correlation coefficients are given for pairs of scalar quantities. Irregular contour intervals (at select percentiles of the data) are used for better visualization. Color scales are bounded by minima and maxima of the data. Minimum and maximum line contours are suppressed. The corresponding spatially unfiltered data are shown in Fig. 10.

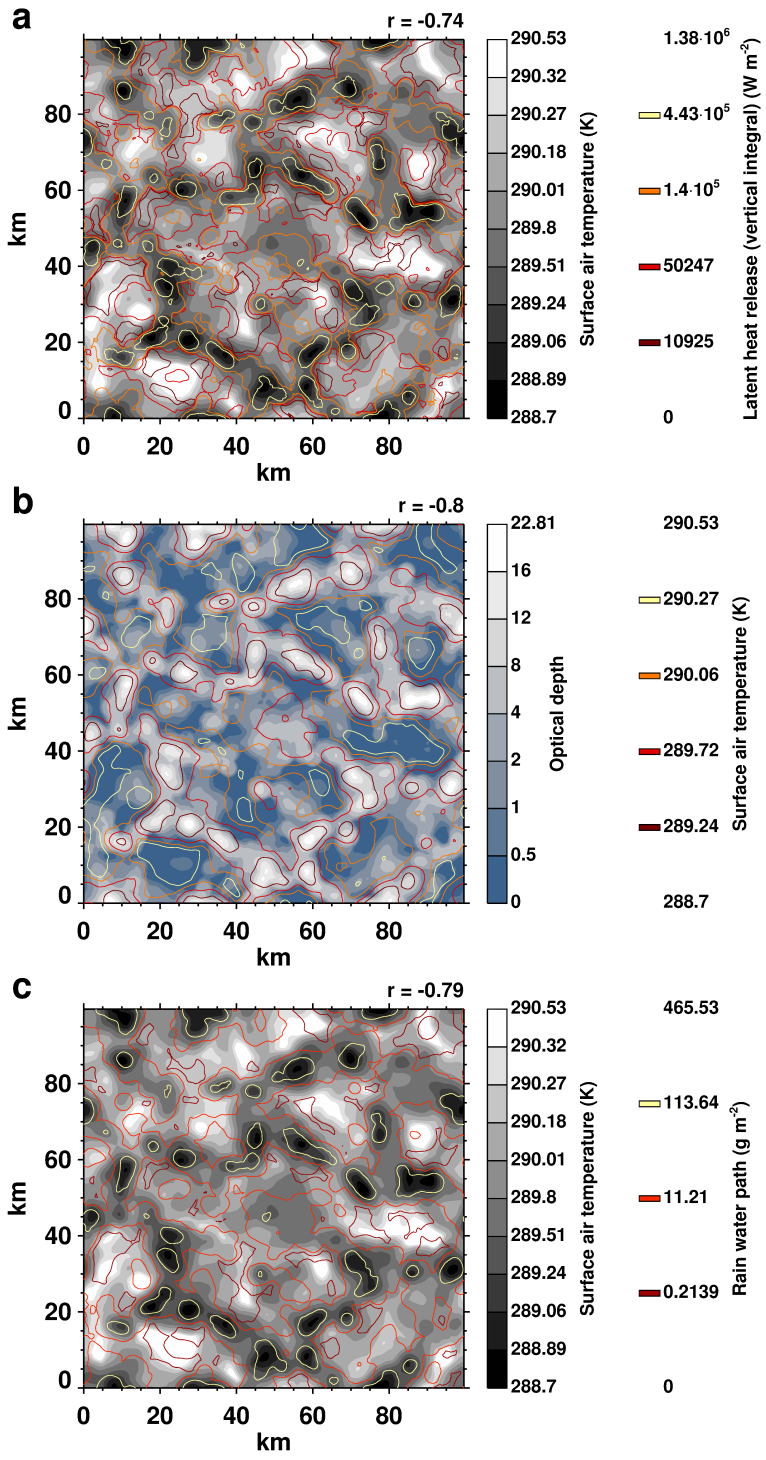

Fig. A-3. Latent heat release path (a), cloud optical depth (b), and rain water path (c) with surface air temperature in simulation $\mathcal{S}_\circ$, after applying a circular low-pass filter with a diameter of 4500 m. Surface air temperature is shown after 26 h, the latent heat release path 40 min, cloud optical depth 30 min, and rain water path 20 min earlier. Correlation coefficients of the data at these lags are given. Irregular contour intervals (at select percentiles of the data) are used for better visualization. Color scales are bounded by minima and maxima of the data. Minimum and maximum line contours are suppressed. The corresponding spatially filtered data are shown in Fig. 11.

B Simulation $\mathcal{S}'_\circ$

Results from simulation $\mathcal{S}'_\circ$ are given here and compared with results from simulation $\mathcal{S}_\circ$.

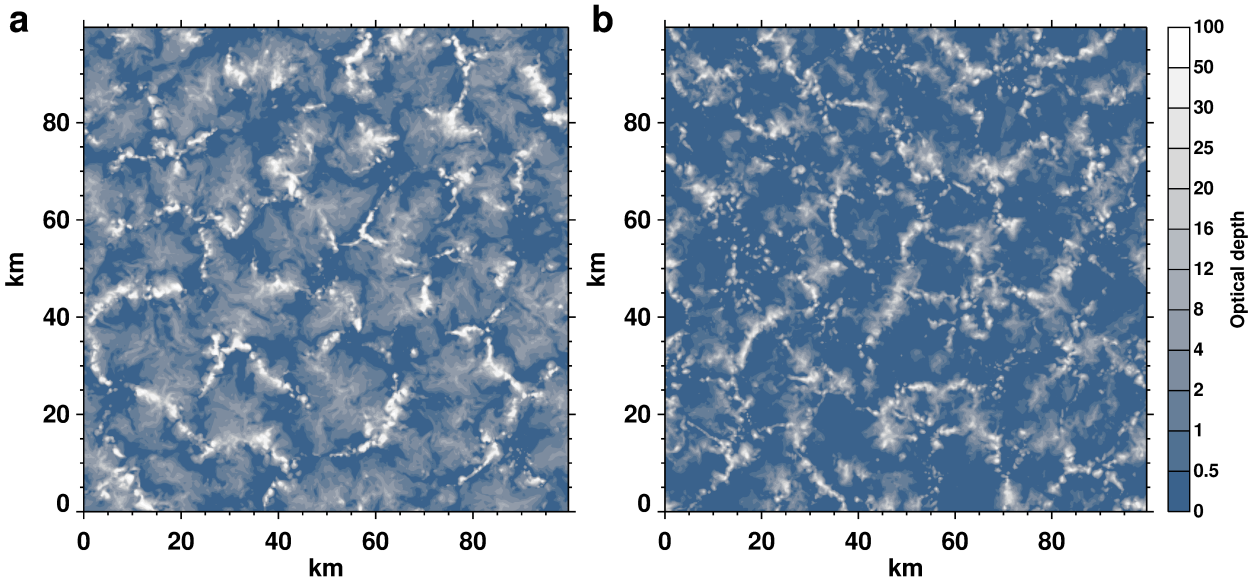

Fig. B-1. Cloud optical depth in simulation $\mathcal{S}'_\circ$ after 12 h (a) and 36 h (b).

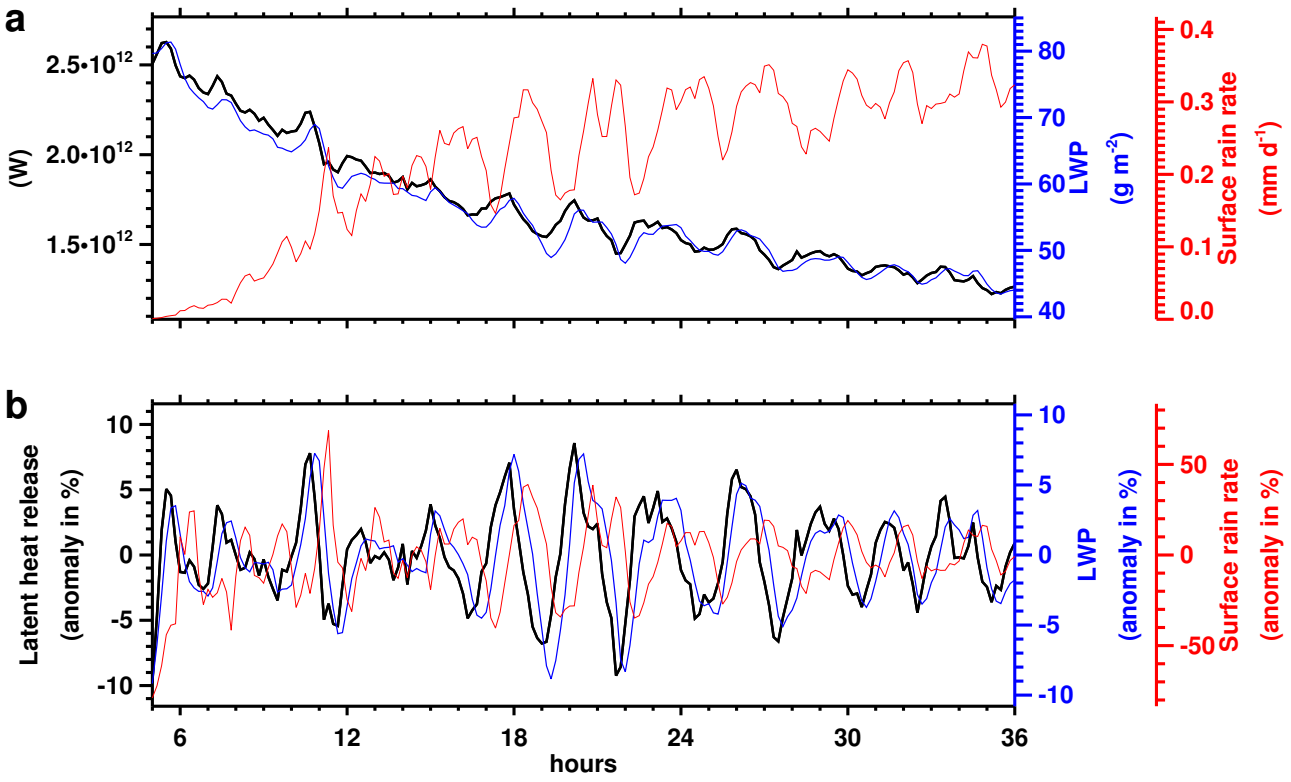

Fig. B-2. (a) domain-integrated latent heat release (heating of the air from condensation of water vapor), domain-averaged liquid water path and surface rain, and (b) their temporal anomalies (against a 3 h running mean) in simulation $\mathcal{S}'_{\circ}$.

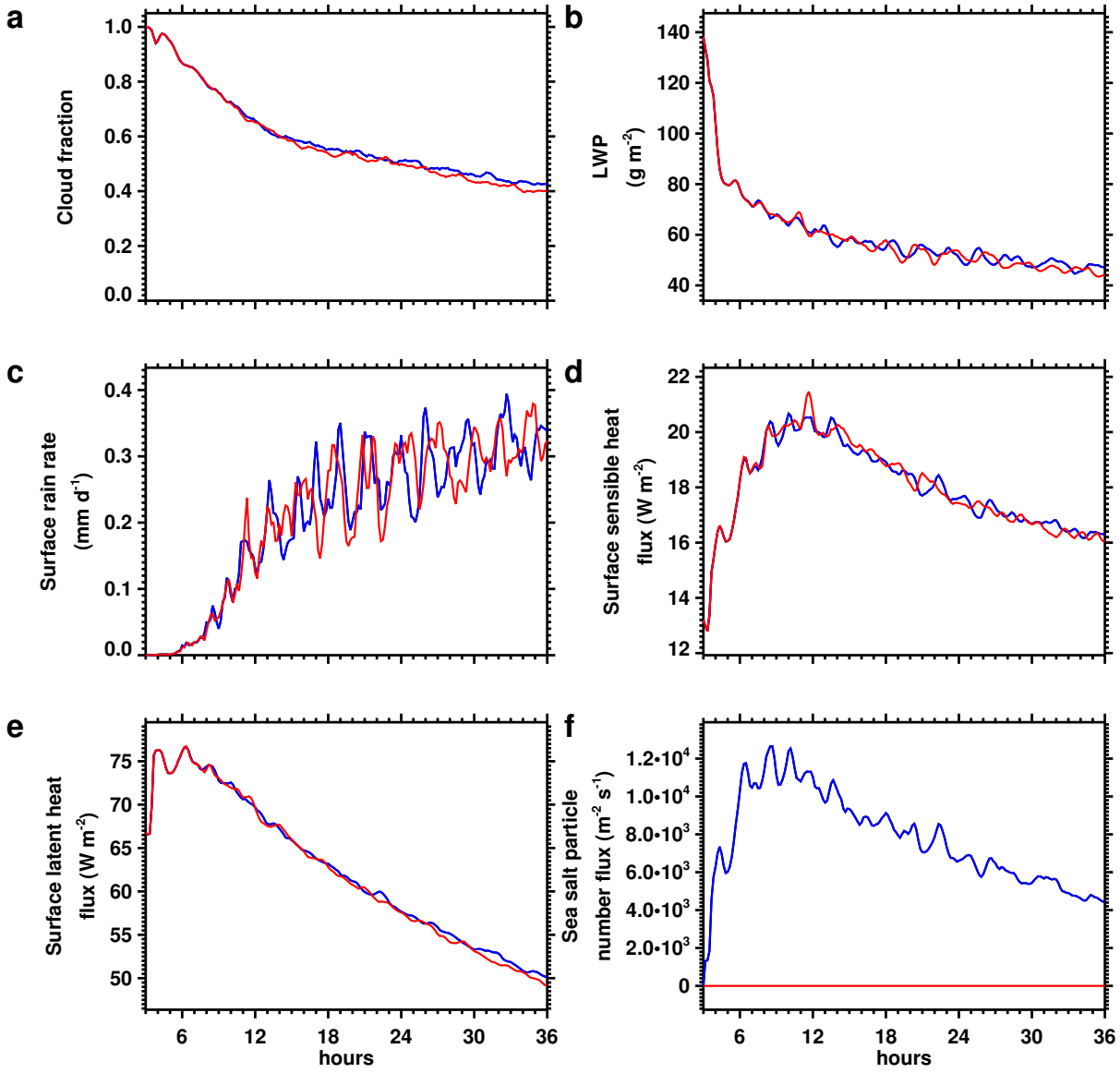

Fig. B-3. Domain-averaged time series of selected quantities in simulation $\mathcal{S}_\circ$ (blue) and $\mathcal{S}'_\circ$ (red).

C Simulation $\mathcal{S}_\circ''$

Results from simulation $\mathcal{S}_\circ''$ are given here and compared with results from simulation $\mathcal{S}_\circ$.

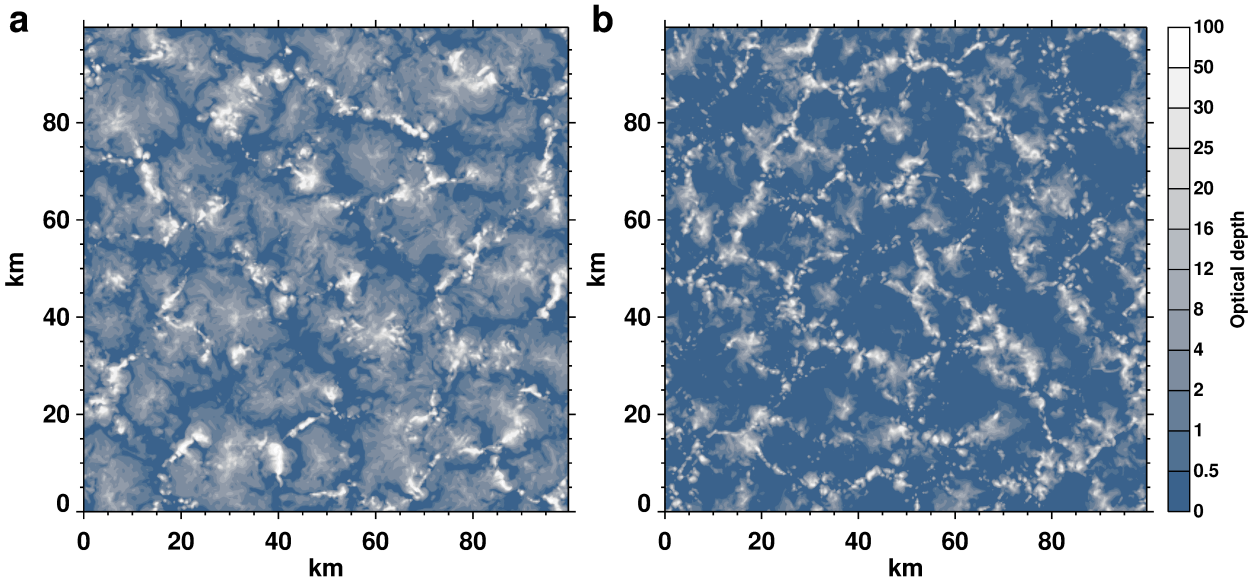

Fig. C-1. Cloud optical depth in simulation $\mathcal{S}_\circ''$ after 12 h (a) and 36 h (b).

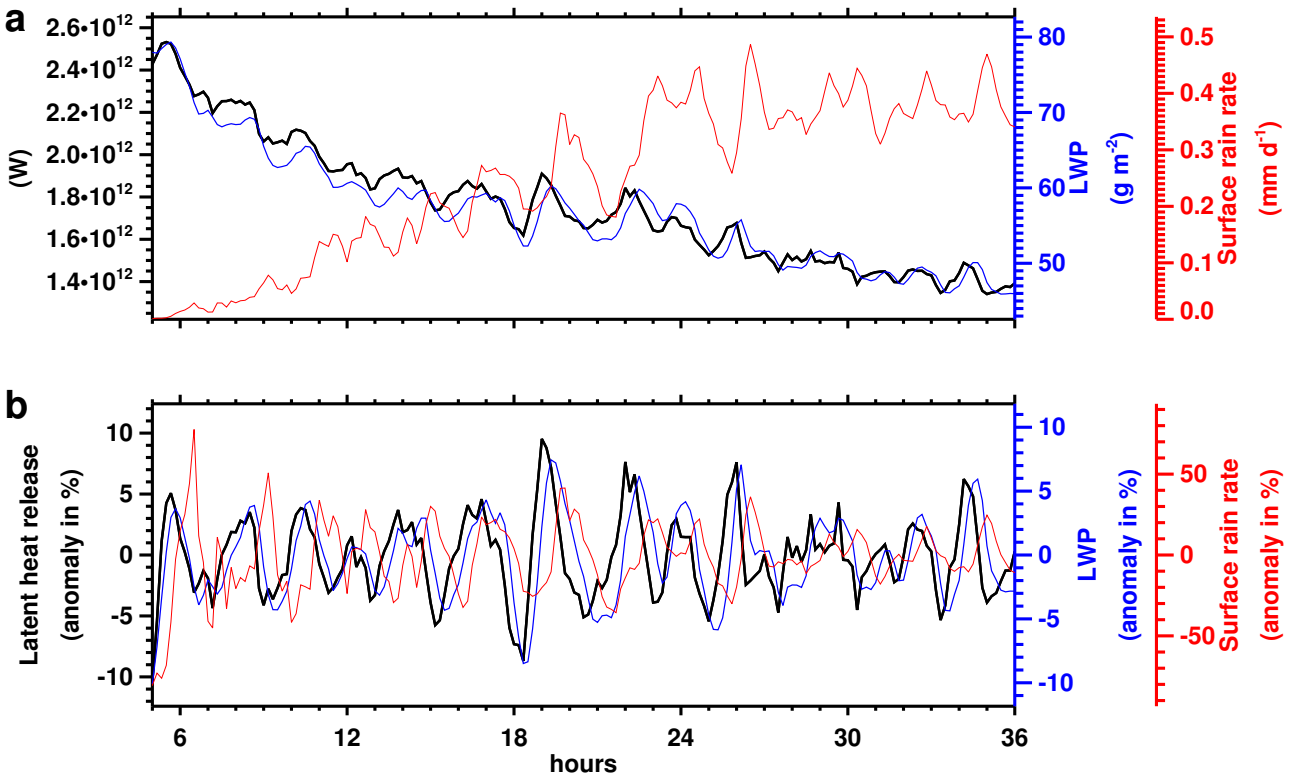

Fig. C-2. (a) domain-integrated latent heat release (heating of the air from condensation of water vapor), domain-averaged liquid water path and surface rain, and (b) their temporal anomalies (against a 3 h running mean) in simulation $\mathcal{S}_{\circ}''$.

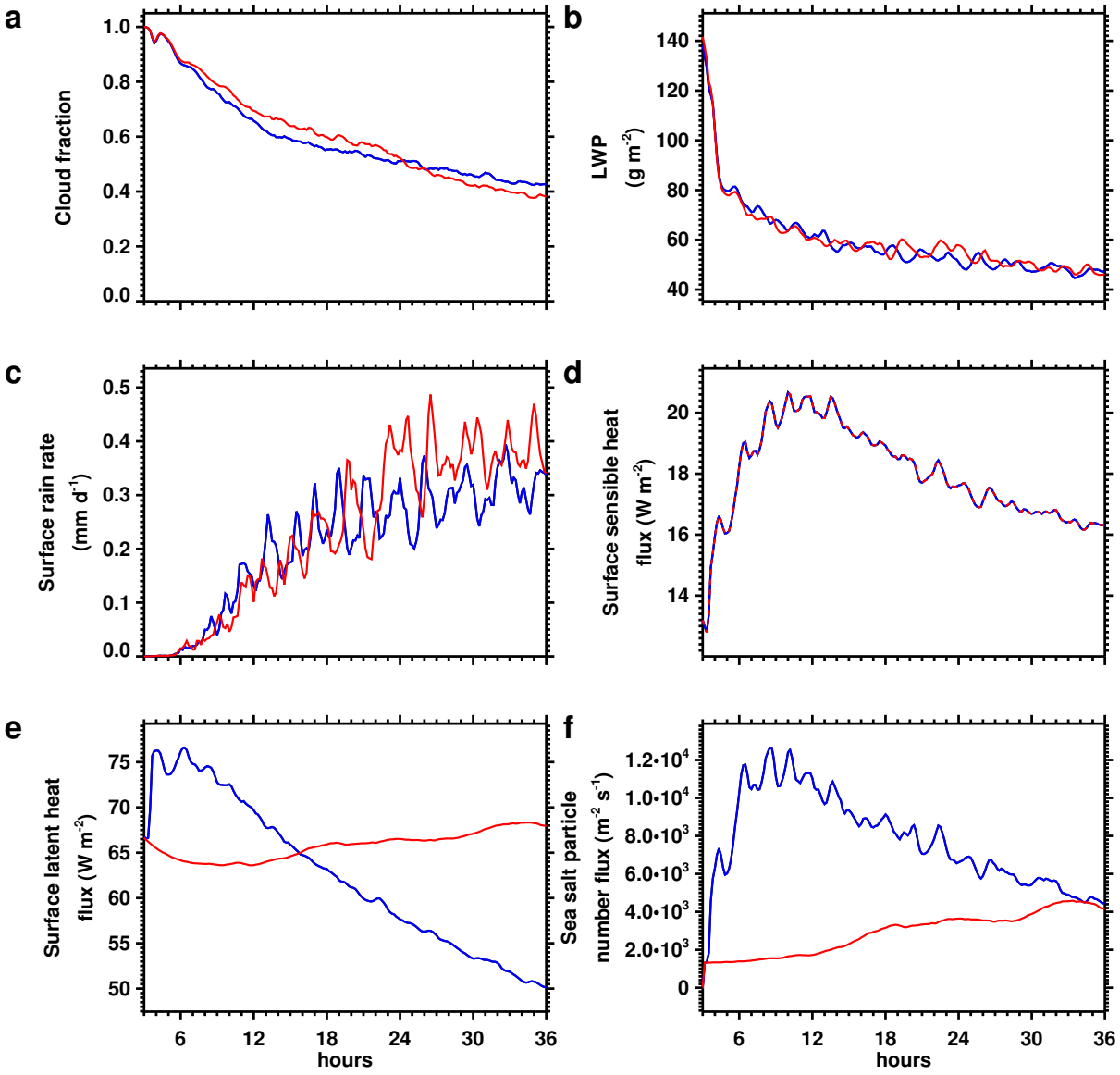

Fig. C-3. Domain-averaged time series of selected quantities in simulation $\mathcal{S}_\circ$ (blue) and $\mathcal{S}''_\circ$ (red).